

RESEARCH

Open Access



Genomic and immunological profiles of small-cell lung cancer between East Asians and Caucasian

Anqi Lin^{1†}, Ningning Zhou^{2†}, Weiliang Zhu^{1†}, Jiexia Zhang³, Ting Wei¹, Linlang Guo⁴, Peng Luo^{1*} and Jian Zhang^{1*}

Abstract

The characterization of immunological and genomic differences in small-cell lung cancer (SCLC) between East Asian (EA) and Caucasian patients can reveal important clinical therapies for EA patients with SCLC. By sequencing and analyzing a molecular and immunological dataset of 98-SCLC patients of EA ancestry, immunogenicity, including DNA damage repair alterations and tumor mutation burden (TMB), was found to be significantly higher in the EA cohort than in the Caucasian cohort. The epithelial-mesenchymal transition (EMT) was the signaling signature with the predominant frequency of mutations across all patients in the EA cohort. Analysis of tumor-infiltrated immune cells revealed that resting lymphocytes were significantly enriched in the EA cohort. Compound-targeting analysis showed that topoisomerase inhibitors might be capable of targeting *TP53* and *RB1* comutations in EA SCLC patients. EA SCLC patients who harbored *COL6A6* mutations had poor survival, while Caucasian SCLC patients with *OTOF*, *ANKRD30B*, and *TECPR2* mutations were identified to have a shorter survival.

Keywords: SCLC, East Asian, Caucasian, Genomic, Immune-infiltrating

Introduction

Small-cell lung cancer (SCLC) accounts for 13~20% of lung cancers and is characterized by rapid growth, expression of neuroendocrine markers, early spread and secondary therapeutic resistance [1–4]. Approximately one-third of patients diagnosed with early-stage disease are commonly cured with standard chemotherapy or radiotherapy, while the majority of patients have only a few treatment options, such as palliative care [3]. The 5-year overall survival (OS) rate for SCLC is extremely low (5–10%) [5]. Several studies have characterized the genomic profile of SCLC and discovered therapeutic

implications and new candidate alterations, such as *BRAF*, *KIT* and *PI3K/AKT/mTOR* [1, 5–8]. Additionally, *NOTCH* family genes, acting as tumor suppressors, are capable of regulating neuroendocrine differentiation involving tumor pathogenesis [1]. Therefore, understanding the key biological signaling pathways may stratify vulnerabilities and define new therapeutic targets. Additionally, previous studies indicated that the majority of SCLC harbors *RB1/TP53* co-mutations, suggesting that inactivation of *RB1* and *TP53* is a prerequisite in SCLC [1, 9]. Thus, further analysis of *RB1/TP53* co-mutations has critical value for characterizing biological features and designing optional treatments.

Recently, immunotherapy, particularly immune checkpoint inhibitors (ICIs), has been incorporated in first-line treatment for SCLC and substantially improves the median survival of SCLC [10]. In addition, ICI efficacy was associated with high tumor immunogenicity,

*Correspondence: luopeng@smu.edu.cn; zhangjian@i.smu.edu.cn

[†]Anqi Lin, Ningning Zhou, Weiliang Zhu and Jiexia Zhang contributed equally to this work

¹ Department of Oncology, Zhujiang Hospital, Southern Medical University, 253 Industrial Avenue, Guangzhou 510282, Guangdong, China
Full list of author information is available at the end of the article



inflammatory expression profiles and immune checkpoint expression [11].

To date, genomic studies of SCLC have focused on a single ancestry (East Asian (EA) or Caucasian patients) [1, 4]. However, SCLC may differ substantially among EA and Caucasian individuals in terms of the genomic characteristics, tumor microenvironment (TME), and critical biological pathways.

To better understand the ancestry disparities among the EA and Caucasian populations and to portray a comprehensive genomic and immunological profile of EA SCLC patients, we sequenced the transcriptomes ($n=59$) and whole exomes ($n=98$) of 98 EA SCLC patients from China. To discover new genomic targets enriched in the EA cohort, we compared our data to published whole-exome sequencing (WES) data of a Caucasian cohort consisting of 45 patients (reported by George et al.) [1] by analyzing the clinical, immunological and genomic features.

Methods

Sample collection, gene sequencing and public dataset processing

The Institutional Review Boards (IRBs) of the First Affiliated Hospital of Guangzhou Medical University, the Sun Yat-sen University Cancer Center, and the Zhujiang Hospital of Southern Medical University approved this study. A total of 98 samples from EA SCLC patients were provided by these hospitals under IRB-approved protocols with informed consent. These 98 tumor samples from EA SCLC patients were collected retrospectively from surgical material. We used blood or adjacent normal tissues as a matched control. TNM stage, sex, smoking history, and age were collected. Detailed information is provided in the Additional file: Supplemental methods 16.

Processed WES data and RNA sequencing (RNA-seq) files of 45 Caucasian SCLC patients from a 2015 Nature study were downloaded from cBioPortal (https://www.cbioportal.org/study/summary?id=sclc_ucologne_2015) [1]. The SCLC cell lines described in this study were derived from the Genomics of Drug Sensitivity in Cancer (GDSC) database [12] and had drug sensitivity and WES data.

Immune profiling analysis

The CIBERSORT algorithm [13] was supplied with mRNA data of EA and Caucasian SCLC patients. The proportion of twenty-two tumor-infiltrating immune cells was used in downstream analysis. Then, expression values were selected for CIBERSORT analysis using default parameters ($\text{perm}=1,000$; $\text{QN}=F$). Marker genes [14, 15] related to immune cells, antigen presentation, cytotoxicity, cytokines, and immune checkpoints were

collected from previous studies and used to evaluate the immune signatures of SCLC. To compare differentially immune cells and immune-related genes, a linear model of the limma package was supplied.

Mutational landscape and DDR-related analysis

The Complexheatmap package [16] was used to visualize the waterfall plot of mutations in EA and Caucasian SCLC patients. Nonsynonymous mutation types were determined using the maftools package [17]. The summary plot of the MAF files and figures of somatic interactions were generated by the maftools package. Tumor mutation burden (TMB) values were calculated according to a previous study [18]. A list of hallmark and DNA damage response (DDR) genes was collected from the Molecular Signatures Database (<https://www.gsea-msigdb.org/gsea/msigdb/index.jsp>) [19] and used for signaling alteration analysis. The DDR signature scores were calculated using the gene set variation analysis (GSVA) package [20] with the single-sample gene set enrichment analysis (ssGSEA) method. According to the median age or TMB value, SCLC patients were classified into groups: older vs young and high TMB vs low TMB. Driver gene annotations were downloaded from the Network of Cancer Genes (NCG) database [21].

Compound-targeting analysis

To identify which inhibitors/compounds may be useful for targeting cells with *TP53* and *RBI* co-mutations, we applied the Broad Institute's Connectivity Map (CMap) build 02 [22], which is a public online analytical tool (<https://portals.broadinstitute.org/cmap/>) that allows the analyzer to predict potential inhibitors/compounds based on upregulated and downregulated genes in a gene expression signature.

To further discover the mechanism of action (MoA) [23] and inhibitors/compounds, we analyzed them using CMap tools (<https://clue.io/>). The CMap method is similar to the gene set enrichment analysis (GSEA) algorithm, which can identify similarities and connectivities (range: -1 to 1) based on differential gene expression data.

Statistical analysis

All analyses were performed in R (version 3.6.1). The Mann–Whitney U test was used for the comparison of two continuous variables. Fisher's exact test was supplied with two categorical variables. P values were controlled for false discovery rate (FDR), and an FDR less than 0.05 was considered statistically significant; all statistical tests were two-sided. Survival analysis was performed using the Kaplan–Meier method, and the log-rank test p-value was calculated. A Cox regression model was used in univariable analyses.

Results

Genomic profile of the EA and Caucasian SCLC cohorts

With the Mutect2 algorithm [24], 103,100 single-nucleotide polymorphisms (SNPs) and 2926 short insertions/deletions (indels) were identified in the EA cohort (Fig. 1a), and the majority were missense mutations (n=92,103). We identified 11,029 SNPs and 676 indels in the Caucasian cohort (Fig. 1b). In particular, C>T was identified predominantly in the EA cohort, whereas

C>A was the predominant single-nucleotide variant (SNV) in the Caucasian cohort (Fig. 1a,b). The top 20 mutated genes in the EA cohort are shown in Fig. 1c and *TP53* (89%), *TTN* (80%), *RB1* (67%), *MUC16* (57%), and *RYR2* (49%) were the most frequently mutated genes. The top 20 mutations in the Caucasian cohort are shown in Fig. 1d, and *TP53* (89%), *TTN* (73%), *RB1* (71%), *LRP1B* (49%), and *MUC16* (49%) were the most frequently mutated genes. We observed higher co-occurrence and

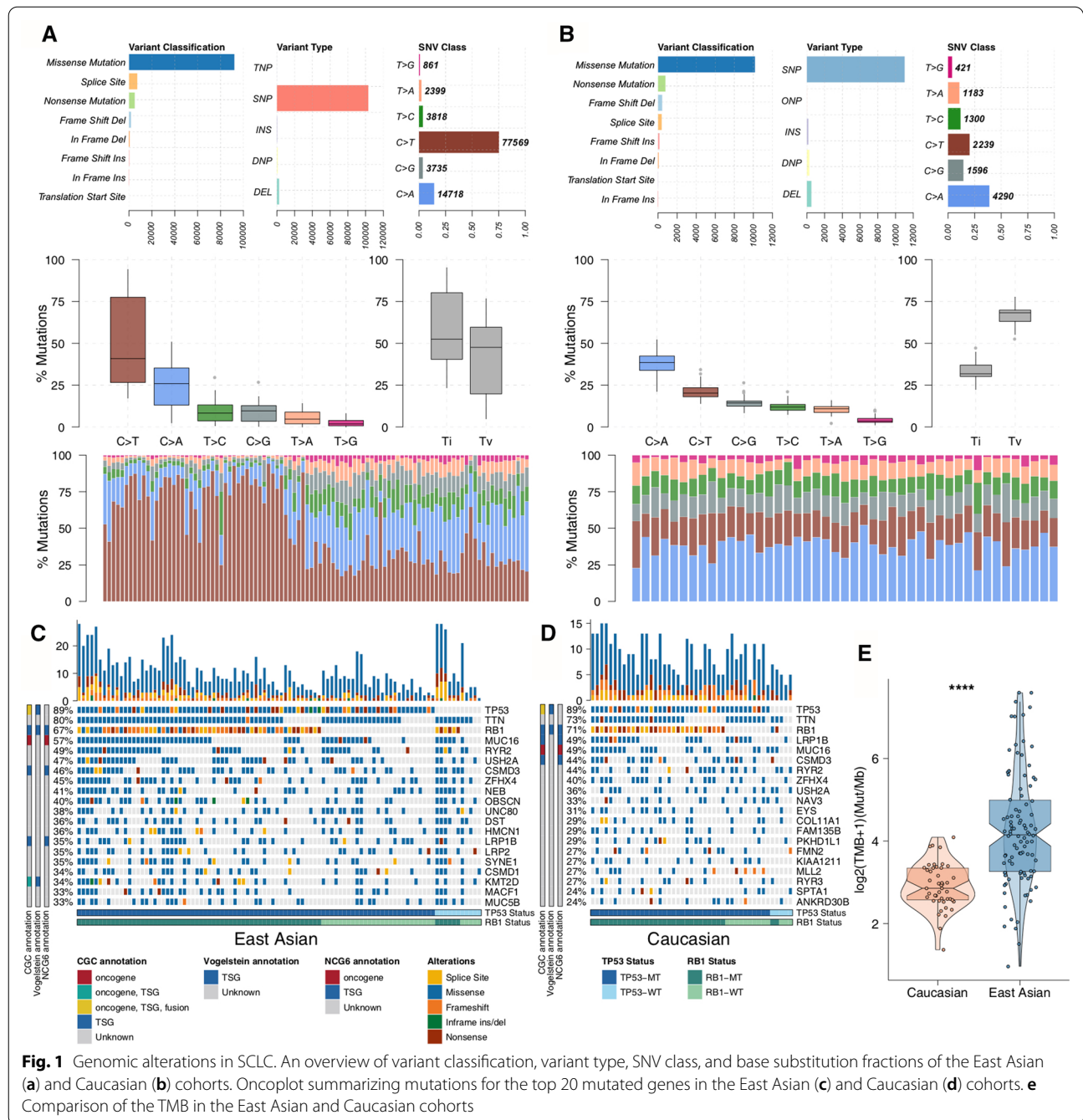


Fig. 1 Genomic alterations in SCLC. An overview of variant classification, variant type, SNV class, and base substitution fractions of the East Asian (a) and Caucasian (b) cohorts. Oncoplot summarizing mutations for the top 20 mutated genes in the East Asian (c) and Caucasian (d) cohorts. e Comparison of the TMB in the East Asian and Caucasian cohorts

exclusiveness gene pairs in the top 20 mutations of the EA cohort than of the Caucasian cohort (Additional file 1: Fig. S1). Oncogenes and tumor suppressor genes (TSGs) play a role in cancer evolution and development. For example, *LRP1B* and *MUC16* exhibited co-occurrence in the EA cohort (Additional file 1: Fig. S1a; Additional file 10: Table S1), while there was no co-occurrence/mutual exclusivity of oncogenes/TSGs in the Caucasian cohort (Additional file 1: Fig. S1b; Additional file 11: Table S2). The TMB was significantly higher in EA SCLC patients than in Caucasian SCLC patients (median 16.75 vs 6.24 per Mb; mean 30.95 vs 7.03 per Mb; $FDR < 0.0001$; Fig. 1e).

***RB1* and *TP53* mutations in SCLC**

Alterations in *RB1* and *TP53* occurred in approximately 65% and approximately 90% of the SCLC patients, respectively [1]. We identified that 59% of patients in the EA cohort had co-occurrent *TP53* and *RB1* mutations; 28% had only a *TP53* mutation, 6% had only an *RB1* mutation, and 7% had no alterations in *TP53* or *RB1* (Fig. 2a). The Caucasian cohort harbored more patients with alterations in both *TP53* and *RB1* (67%), although there was no significant difference between cohorts. In the EA cohort (Fig. 2b), multiple missense mutations occurred in the DNA-rich and tetramerization domains, while truncating mutations in *RB1* affected the DUF3452 and RB B, RB A and RB C domains. Similarly, *RB1* and *TP53* mutations affected the same domain in the Caucasian cohort (Fig. 2c). Subsequently, we explored the association between *RB1* and *TP53* mutations and the survival of SCLC patients. In the EA cohort, *TP53*, *RB1*, and *TP53/RB1* co-mutations exhibited no significant associations with a survival benefit (Fig. 2d). In addition, there were no correlations between survival and alterations in *RB1*, *TP53* or both *RB1* and *TP53* in the Caucasian cohort (Fig. 2e).

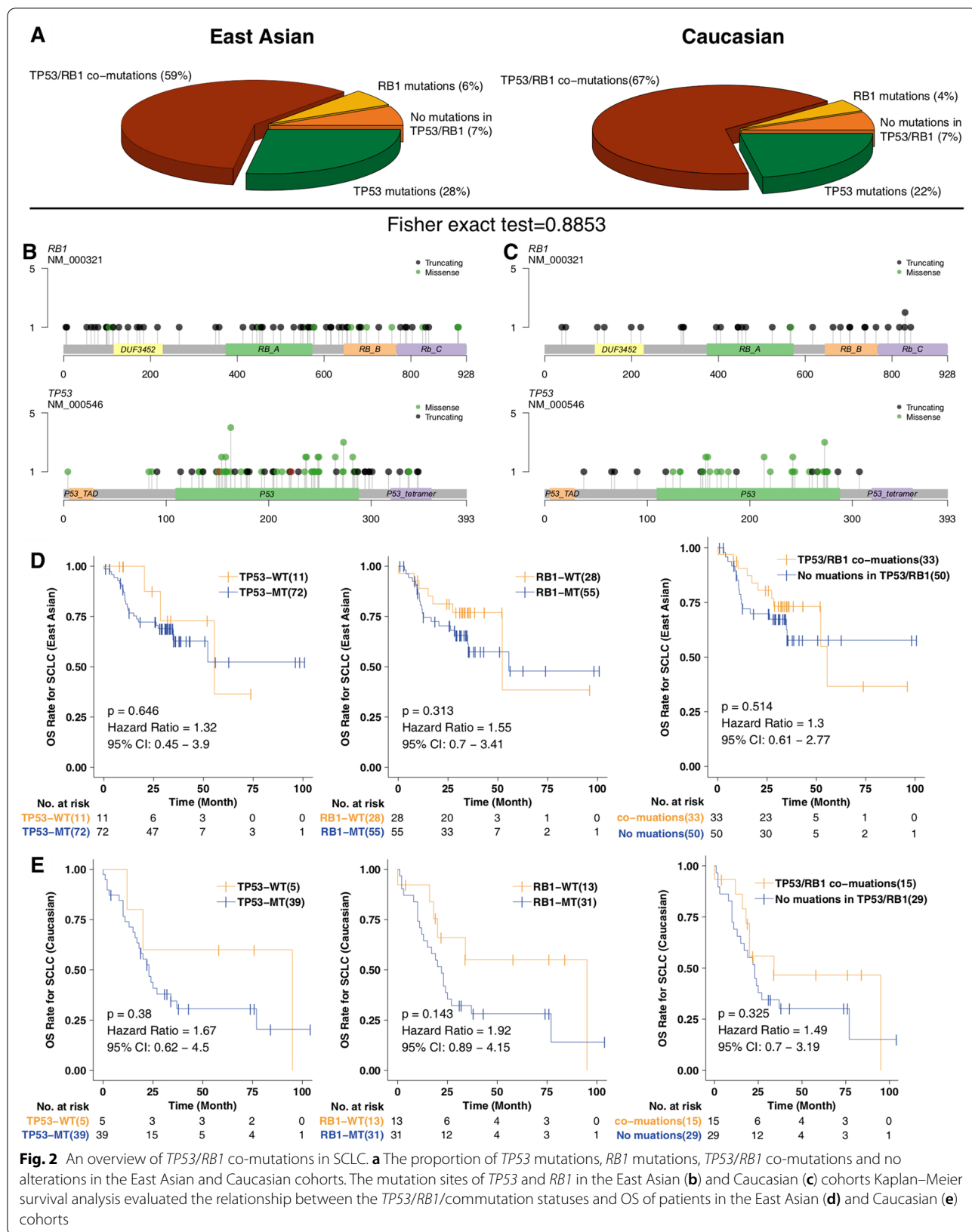
Hallmark pathway alterations and significantly mutated drivers

For each SCLC patient, we calculated the frequency of patients harboring at least 1 alteration in each of the 28 signaling pathways in both the EA and Caucasian cohorts (Fig. 3a–b). Epithelial-mesenchymal transition (EMT) was the signaling pathway that was most frequently mutated (10.2% of all alterations) across all patients in the EA cohort, followed by *E2F* targets, *KRAS* signaling, *P53* signaling, *IL2/STAT5* signaling, hypoxia, adipogenesis, interferon-gamma response, and inflammatory response pathways, which were altered in 8.9%, 7.4%, 7.4%, 7.0%, 6.6%, 6.5%, 6.4% and 6.2% of all alterations, respectively. In contrast, reactive oxygen species pathways harbored the lowest number of alterations (Fig. 3a). Alterations in

EMT signaling were identified most predominantly in the Caucasian cohort, while only some genes were altered in the angiogenesis and reactive oxygen species signaling pathways. More detailed information on the mutation frequencies of hallmark pathways is shown in Fig. 3b. Subsequently, with annotations from the Network of Cancer Genes (NCG) database, we compared the differences in frequencies of driver genes between the EA and Caucasian cohorts. Of the 42 significantly mutated genes between the two cohorts (all $p < 0.05$; Fig. 3c), TSGs were commonly involved (up to 54.8%). For alterations commonly found in the EA cohort, TSGs, such as *FAT1*, *NCOR2*, *SMARCA4*, *UBR5*, and *CREBBP*, showed higher alteration rates, while *ARHGEF10* exhibited a lower alteration rate than those found in the Caucasian cohort. Additionally, a well-known oncogene (*EGFR*) had higher numbers of alterations (mainly missense mutations) in the EA cohort than in the Caucasian cohort, followed by other oncogenes (*TRRAP*, *MTOR*, *TNC*, *DNMT1*, and *RET*). For mutual exclusivity and co-occurrence driver analyses, alterations in *MTOR*, *SPEN*, *NCOR1*, *BRCA2*, *POLE*, *EGFR*, *ARID1B*, and some other genes frequently co-occurred in the EA cohort (Additional file 2: Fig. S2a; Additional file 12: Table S3), whereas there were no significant mutual exclusivity gene pairs. In contrast, there were a few comutated gene pairs, namely, *BRCA2*, *FANCA* and *ZMYM3*, in the Caucasian cohort (Additional file 2: Fig. S2b; Additional file 13: Table S4).

DNA damage repair pathway alterations and correlation with TMB

Mutations in DDR pathways have been identified to affect the efficacy of platinum-based chemotherapy and immunotherapy for SCLC. For each DDR pathway, we computed the alteration frequencies of SCLC samples with at least 1 mutation in each of 8 signaling pathways (Fig. 4a–b). Homologous recombination (HR) was the pathway harboring the highest alteration frequencies among total mutations (32.2%), followed by single-strand breaks (SSB; 29.5%) and nucleotide excision repair (NER; 28.3%). However, nonhomologous end joining (NHEJ) pathways harbored the lowest fraction of alteration frequencies in the EA cohort (Fig. 4a). Next, we applied the same analytic pipeline in the Caucasian cohort. Genomic alterations in SSB signaling were highest, while mutations in base excision repair (BER) were the lowest (Fig. 4b). Additionally, some pathways, such as SSB and NHEJ, had mutations distributed among each SCLC patient in either the EA or Caucasian cohort (Fig. 4a, b). Additionally, the number of alterations in each DDR signaling pathway was higher in the EA cohort than in the Caucasian cohort (all adjusted $p < 0.05$; Fig. 4c). Next, we discovered that there was a significantly positive correlation between TMB



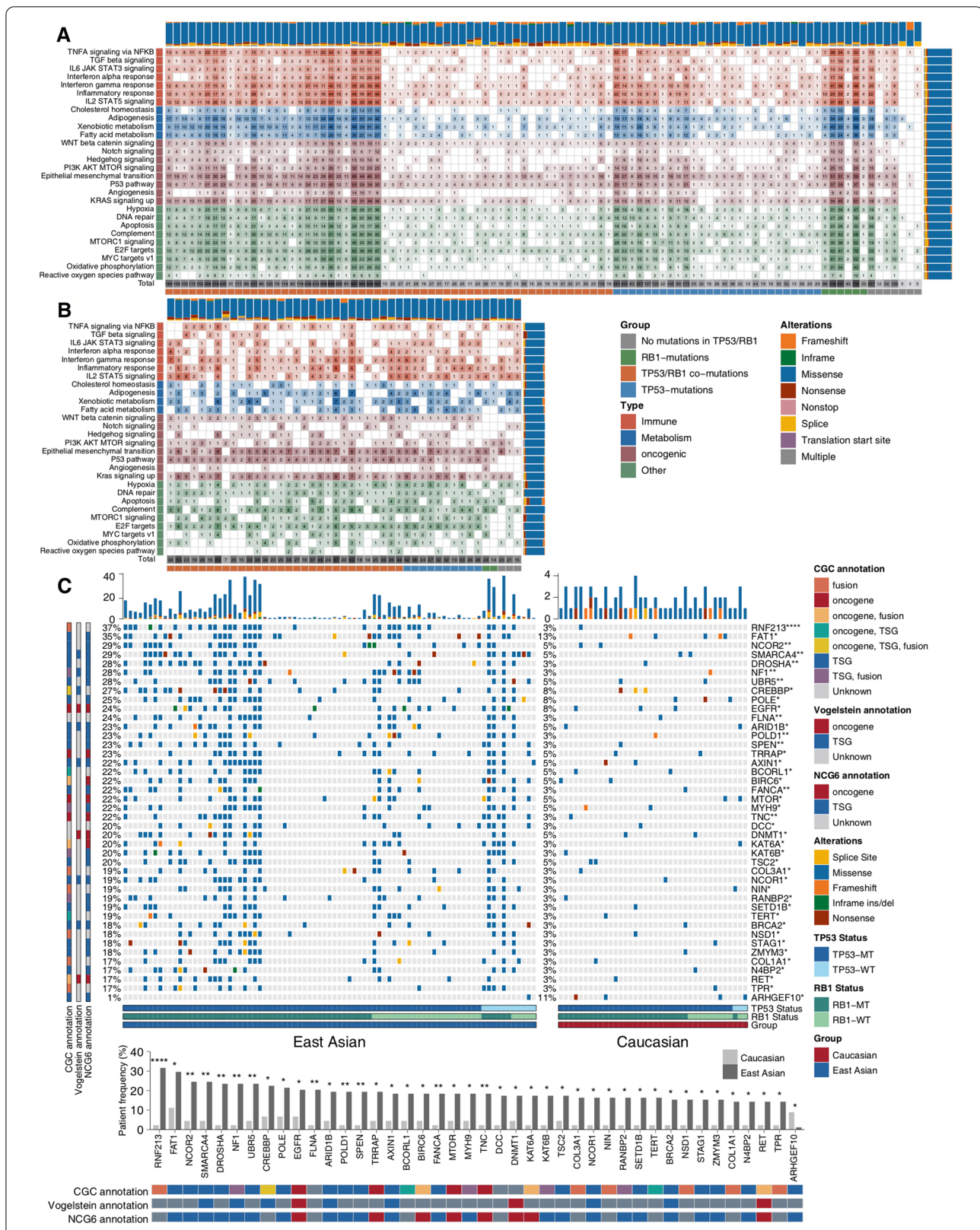
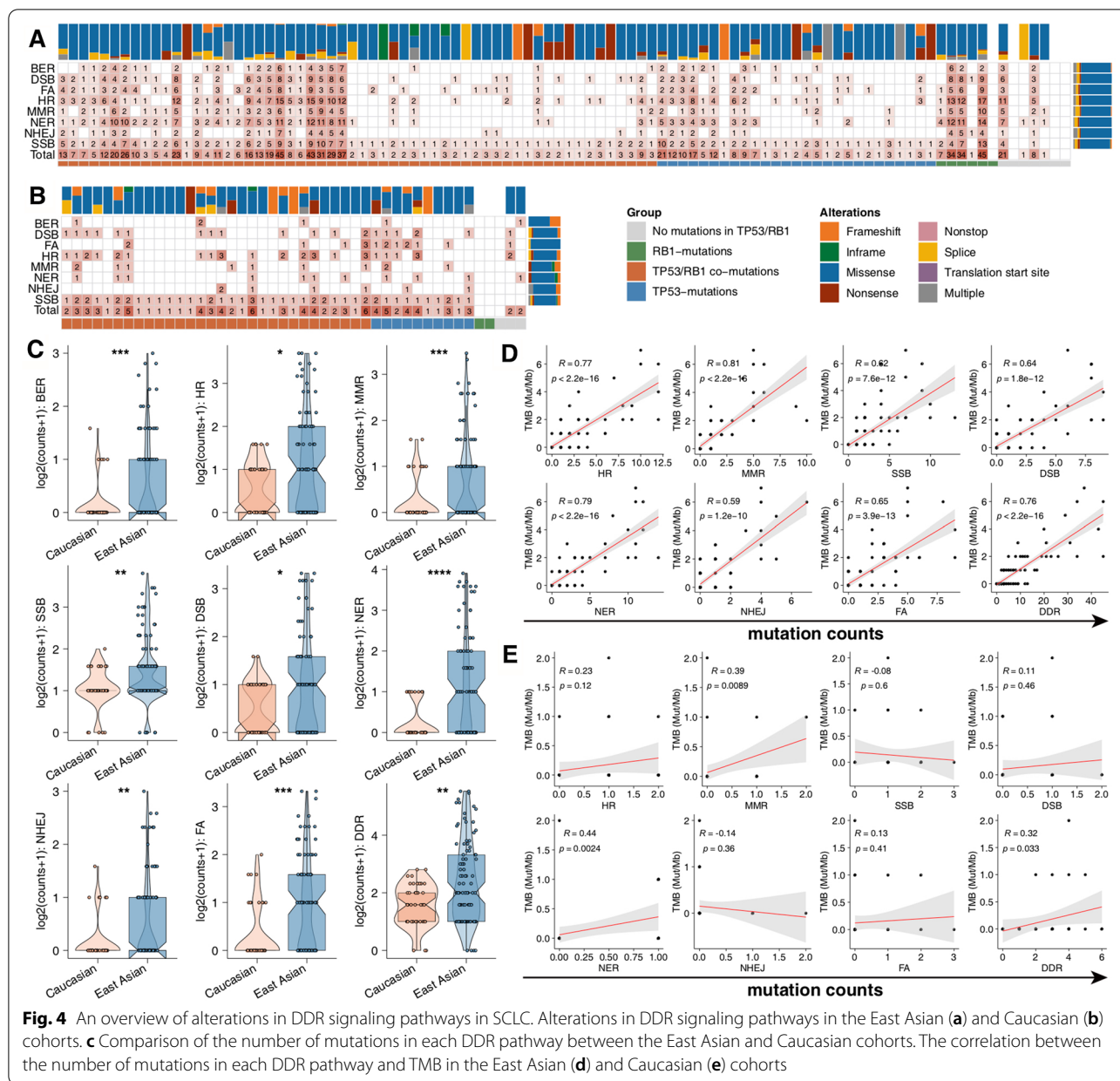


Fig. 3 Genomic alterations in key biological signaling pathways in the East Asian (a) and Caucasian (b) cohorts. c Significantly mutated driver genes in the East Asian and Caucasian cohorts



and each DDR signaling pathway mutations ($p < 0.05$; Fig. 4d). By contrast, we discovered that only NER and DDR mutations were significantly related to higher TMB in the Caucasian cohort (Fig. 4e). Based on the ssGSEA method, none of the DDR signaling pathway alterations were significantly correlated with TMB in both the EA and Caucasian cohorts (Additional file 3: Fig. S3a–b).

Significantly altered genes in key pathways, driver gene landscape and correlation with clinical benefit

The top twenty altered driver genes of the EA and Caucasian cohorts are characterized in Fig. 5a–b. We

discovered up to 60% TSGs were driver genes in the EA cohort (Additional file 4: Fig. S4a), especially the top 5 altered mutations (*TP53*, *RB1*, *CSMD3*, and *LPR1B*). Up to 25% of oncogenes were commonly altered in the Caucasian cohort (Additional file 4: Fig. S4b), including *MUC16* (50%), *PREX2* (16%), *ZNF521* (14%), *ALK* (11%), *CTNND2* (11%) and *MUC4* (11%). Particularly interesting alterations across the EA and Caucasian cohorts were *TP53* and *RB1*. The main alteration type of *TP53* in the EA cohort was missense mutations (66.0%), followed by nonsense mutations (16.0%) and frameshift mutations (9.6%). In the Caucasian cohort, *TP53* was commonly

altered as missense mutations (69.0%) and frameshift mutations (16.7%). In the EA cohort, *RB1* was frequently altered as frameshift mutations (31.5%), followed by nonsense mutations (28.8%), splice sites (23.3%), and missense mutations (16.4%). *RB1* had nearly equal distribution of the three mutation types (37.5% nonsense mutations, 31.3% splice site mutations and 28.1% frameshift mutations) in the Caucasian cohort. Through exploring significant alterations of key pathways, we combined several hallmark pathways and their genes to map nonsynonymous mutations. Multiple genes of each of the five pathways (DNA repair, EMT, G2M checkpoint, hypoxia, and *KRAS* signaling pathways) were significantly mutated in the EA and Caucasian cohorts (Additional file 4: Fig. S4c). For example, in the G2M checkpoint signaling pathway, mutations in TSGs, including *POLE* (26% vs 10%), *BRCA2* (19% vs 3%) and *STAG1* (19% vs 3%), occurred more commonly in the EA cohort than in the Caucasian cohort (all Fisher's exact test $p < 0.05$). We identified *EGFR*, a well-known oncogene, as being mutated at a higher rate in EA patients than in Caucasian patients (25% vs 10%, Fisher's exact test $p < 0.05$). *IGFBP2*, a protein in the EMT signaling pathway, was significantly more mutated in the Caucasian cohort than in the EA cohort (20% vs 4%, $p < 0.05$). Subsequently, we analyzed the potential association among driver genes, clinical phenotypes, and survival of SCLC patients using univariable Cox regression models. In the EA cohort, alterations in *APC*, *NSD3*, *KDM5C*, *CNTRL*, *GRM3*, *CTNND1*, *FANCG*, *MET*, and *SRGAP3* were associated with a significantly poor survival, but mutations in *TP53* or *RB1* conferred no survival benefits (Additional file 5: Fig. S5a). Subsequently, we identified two different driver genes (*FCRL4* and *PTPRT*) to stratify the Caucasian SCLC patients with the same analytical model (Additional file 5: Fig. S5b). However, alterations in *TP53* or *RB1* exhibited no potential associations with patient survival in the Caucasian cohort. Furthermore, we discovered four alterations with totally different prognosis values in the EA and Caucasian cohorts. For instance, driver gene mutations in *OTOF*, *ANKRD30B*, and *TECPR2* correlated with significantly shorter survival in the Caucasian cohort (Additional file 5: Fig. S5c), but these mutations showed no survival benefits in the EA cohort (Additional file 5: Fig. S5d). In contrast, alterations in *COL6A6* were associated with poor OS in EA SCLC patients (Additional file 5: Fig. S5d), while this mutation had no correlation with OS in Caucasian patients (Additional file 5: Fig. S5c).

CMap algorithm identifies potential inhibitors/compounds associated with co-mutations in *RB1* and *TP53*

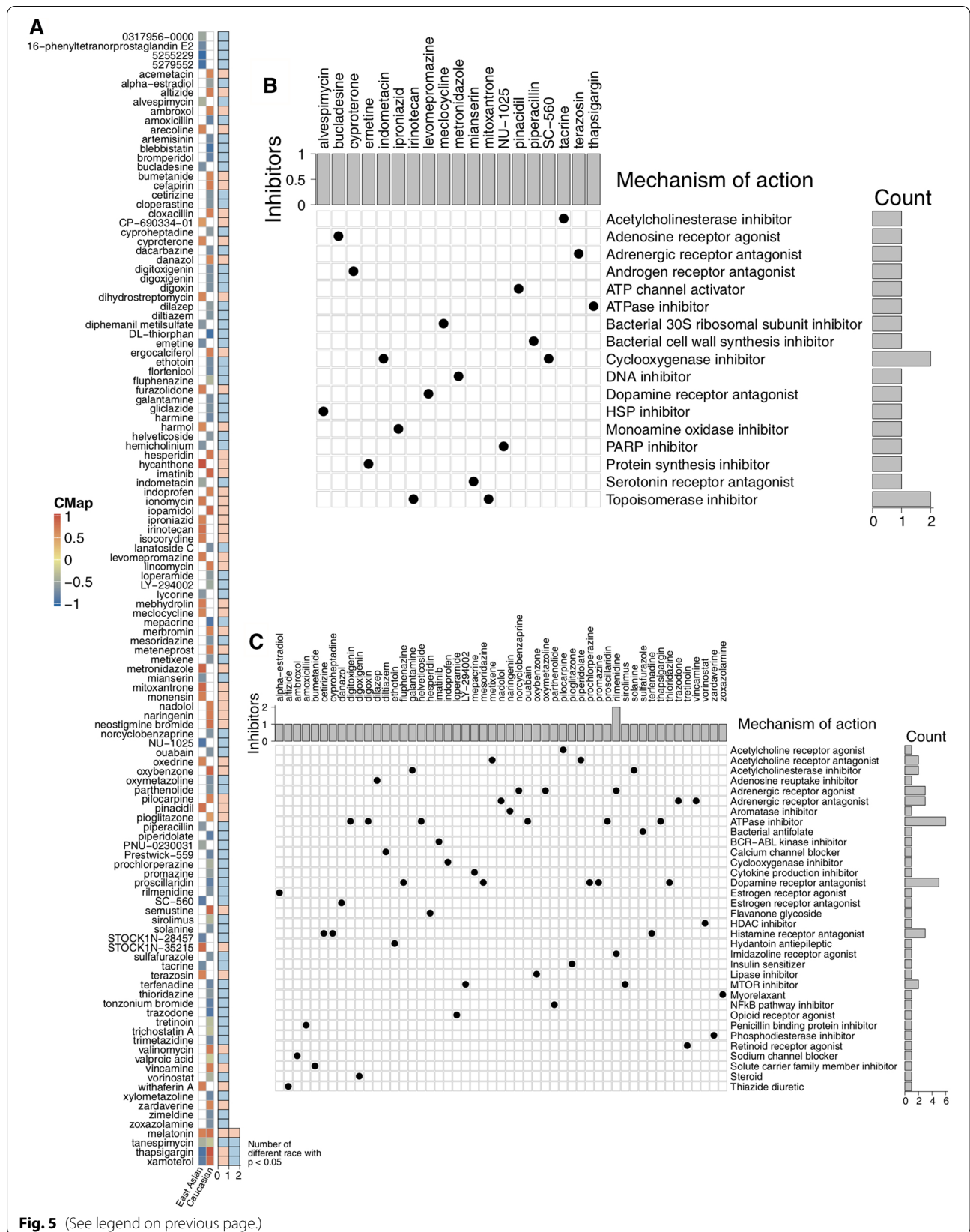
We applied the CMap algorithm for identifying associations among different groups and conditions to discover potential inhibitors/compounds targeting signaling pathways correlated with co-mutations in *TP53* and *RB1* (Fig. 5a; Additional file 14: Table S5, Additional file 15: Table S6). The adrenergic receptor antagonist terazosin, the ATP channel activator pinacidil, the topoisomerase inhibitors mitoxantrone and irinotecan, the heat shock protein (HSP) inhibitor alvespimycin, and the PARP inhibitor (PARPi) NU-1025 showed significant correlations with *TP53* and *RB1* co-mutations in the EA cohort. We identified two compounds, the NF κ B pathway inhibitor parthenolide and the ATPase inhibitor thapsigargin, that were significantly enriched in *TP53* and *RB1* co-mutations in the Caucasian cohort, but these inhibitors exhibited significantly negative correlations with *TP53* and *RB1* co-mutations among the EA cohort. Subsequently, applying CMap MoA analysis to the EA (Fig. 5b) and Caucasian cohorts (Fig. 5c), we discovered 17 mechanisms shared by 19 inhibitors/compounds in the EA cohort (Fig. 5b). Two compounds (irinotecan and mitoxantrone) shared MoAs of topoisomerase inhibitor. We identified SC-560 and indometacin as cyclooxygenase inhibitors. In the Caucasian cohort (Fig. 5c), we found 34 mechanisms shared by 51 inhibitors/compounds, such as dopamine receptor antagonists (thioridazine, promazine, and prochlorperazine), ATPase inhibitors (proscillaridin, thapsigargin, ouabain, digoxin, helveticoside, and digitoxigenin), MTOR inhibitors (sirolimus and LY-294002) and an NF κ B pathway inhibitor (parthenolide). Additionally, we calculated the drug sensitivity associated with more than two mutations from the top 20 mutated genes in the EA and Caucasian cohorts (Additional file 6: Fig. S6a, b).

Immune profile analysis

CIBERSORT, an algorithm to evaluate the fractions of 22 immune cells, was applied to characterize the proportion of tumor-infiltrated immune cells in the EA and Caucasian cohorts. In total, 16 immune cells among the EA and Caucasian cohorts were characterized to be significantly different (Fig. 6a). For example, several immune cells, such as naïve B cells, naïve CD4+ T cells, resting memory CD4+ T cells, resting natural killer cells (NKs), monocytes, activated dendritic cells (DCs), eosinophils, and neutrophils, were significantly enriched in the EA populations, while

(See figure on next page.)

Fig. 5 Correlation of *TP53/RB1* co-mutations with drug sensitivities: CMap analysis. **a** Heatmap showing the enrichment score (positive in blue, negative in red) of each compound from CMap for each cancer type. Compounds are sorted from right to left by descending number of cancer types significantly enriched. Heatmap showing each compound (perturbagen) from the CMap that shares MoAs (rows) and sorted by descending number of compounds with shared MoAs in the East Asian (**b**) and Caucasian (**c**) cohorts



some cells, such as plasma cells, CD8+ T cells, activated memory CD4+ T cells, activated NKs, M1-type macrophages, M2-type macrophages, resting DCs and activated mast cells, accounted for significantly more immune cells in the Caucasian cohort than in the EA cohort. In addition, we compared the differences in the immune-infiltrated signature between the EA and Caucasian cohorts. The mean differences (log fold change) in the 22 immune cells between clinical and genomic features in the EA and Caucasian cohorts are shown in Additional file 7: Fig. S7a, b. Figure 6b shows the mean differences (log fold change) in immune-related mRNA expression levels between EA and Caucasian SCLC patients. Several inhibitory mediators, such as *VEGFA*, *TGFB1*, and *FOXP3*, were significantly upregulated in EA SCLC patients, but some antigen presentation genes, such as *MICA*, *MICB*, and *TAP1*, were significantly downregulated in the EA cohort. Additionally, chemokines (*CXCL9* and *CXCL10*) and cytolytic activity-related genes (*GZMB*) were commonly downregulated in the EA cohort. The mean differences (log fold change) in the clinical and genomic features of immune-related genes in the EA and Caucasian cohorts are shown in Additional file 8: Fig. S8a, b. Notably, among the immune checkpoint-related genes in both the EA and Caucasian cohorts, we discovered that two genes (*PDCD1* and *HAVCR2*) were significantly enriched in the Caucasian cohort compared with the EA cohort (Fig. 6c). The correlation analysis between the TMB, DDR, and immune cells in the EA and Caucasian cohort was shown in Additional file 9: Fig. S9. In the Caucasian cohort, we found that there was a positive correlation between the proportions of the activated NK cells and the DDR mutation counts or TMB. Similarly, the abundance of the activated DCs was positively associated with the DDR or, SSB, or MMR mutation counts. The proportion of the follicular helper T cells was positively correlated with the TMB (Additional file 9: Fig. S9a). In the EA cohort, there was a negative correlation between the proportion of the monocytes and the HR, DSB, NHEJ, FA, or DDR mutation counts. Additionally, we found that the abundance of the resting NK cells was positively correlated with the BER mutation counts (Additional file 9: Fig. S9b).

Discussion

Here, we performed a comprehensive clinical, genomic, and immunological analysis based on the WES and transcriptome data in EA SCLC patients and further compared the results with a previously published dataset of Caucasian SCLC patients (reported by George et al.). We identified that *LRP1B* and *MUC16* were co-occurrent in the EA cohort, while there was no co-occurrence/mutual exclusivity of oncogenes/TSG in the Caucasian cohort. *LRP1B* plays a critical role in cell adhesion, focal adhesion, and tight junction disruption and further inhibits tumor cell migration and proliferation [25–27]. *MUC16*, a well-known mechanical barrier gene, serves as a serum biomarker among various cancers [28]. Ge et al. found that mutations in a panel of five genes, including mutations in *LRP1B* and *MUC16*, predicted poor survival in colorectal cancer, and *LRP1B* and *MUC16* mutations may be involved in tumor metastasis by regulating focal adhesion and cell adhesion [29]. Furthermore, there were no significant differences in the mutation frequencies of two known alterations (e.g., *TP53* and *RBI*) between the EA and Caucasian cohorts.

In the EA SCLC cohort, the number of alterations in gene related to EMT signaling were the highest among the critical biological signaling pathways. Through the EMT mechanism, cancer cells can obtain a motile phenotype, mediate tumor cell metastasis and secondary resistance to common chemotherapies or targeted treatments [30]. Additionally, EMT is associated with poor survival in SCLC [30, 31], and EMT plays a key role in the activation of several oncogenic signaling pathways, such as TGFβ/Akt and MET signaling pathways [30–32]. *CREBBP* mutation rates were notably higher (27%) in the EA cohort than in the Caucasian cohort (8%). *CREBBP* acts as an ubiquitous transcriptional coactivator and histone modifier [1, 33], and *CREBBP* inactivation can promote cell growth in SCLC [33]. Importantly, *CREBBP* is frequently mutated in SCLC [34]. Moreover, treatment with pracinostat, a histone deacetylase inhibitor (HDACi), can increase E-cadherin and acetylated *H3K27*, further reversing the function of *CREBBP* mutations [35, 36]. Additionally, significantly higher mutation rates were identified for *EGFR* in EA SCLC tumors (25%) than in the Caucasian tumors (10%). Studies have found that EGFR tyrosine kinase inhibitor (TKI)-resistant tumors transformed from non-small cell lung cancer (NSCLC) into

(See figure on next page.)

Fig. 6 Immunological profiles in SCLC. **a** The difference in the contents of immune cells (CIBERSORT) between the East Asian and Caucasian cohorts. **b** Heatmap depicting the mean differences in immune-related gene mRNA expression levels between the East Asian and Caucasian SCLC cohorts. The y-axis indicates tumor-infiltrating leukocytes, immune signatures, or gene names. Each square represents the fold change or difference in each indicated tumor-infiltrating leukocyte, immune signature, or immune-related gene between the East Asian and Caucasian SCLC cohorts. Red indicates upregulation, while blue indicates downregulation. **c** The expression levels of immune checkpoints in the East Asian SCLC cohort versus the Caucasian SCLC cohort (*P < 0.05; **P < 0.01; ***P < 0.001; ****P < 0.0001)

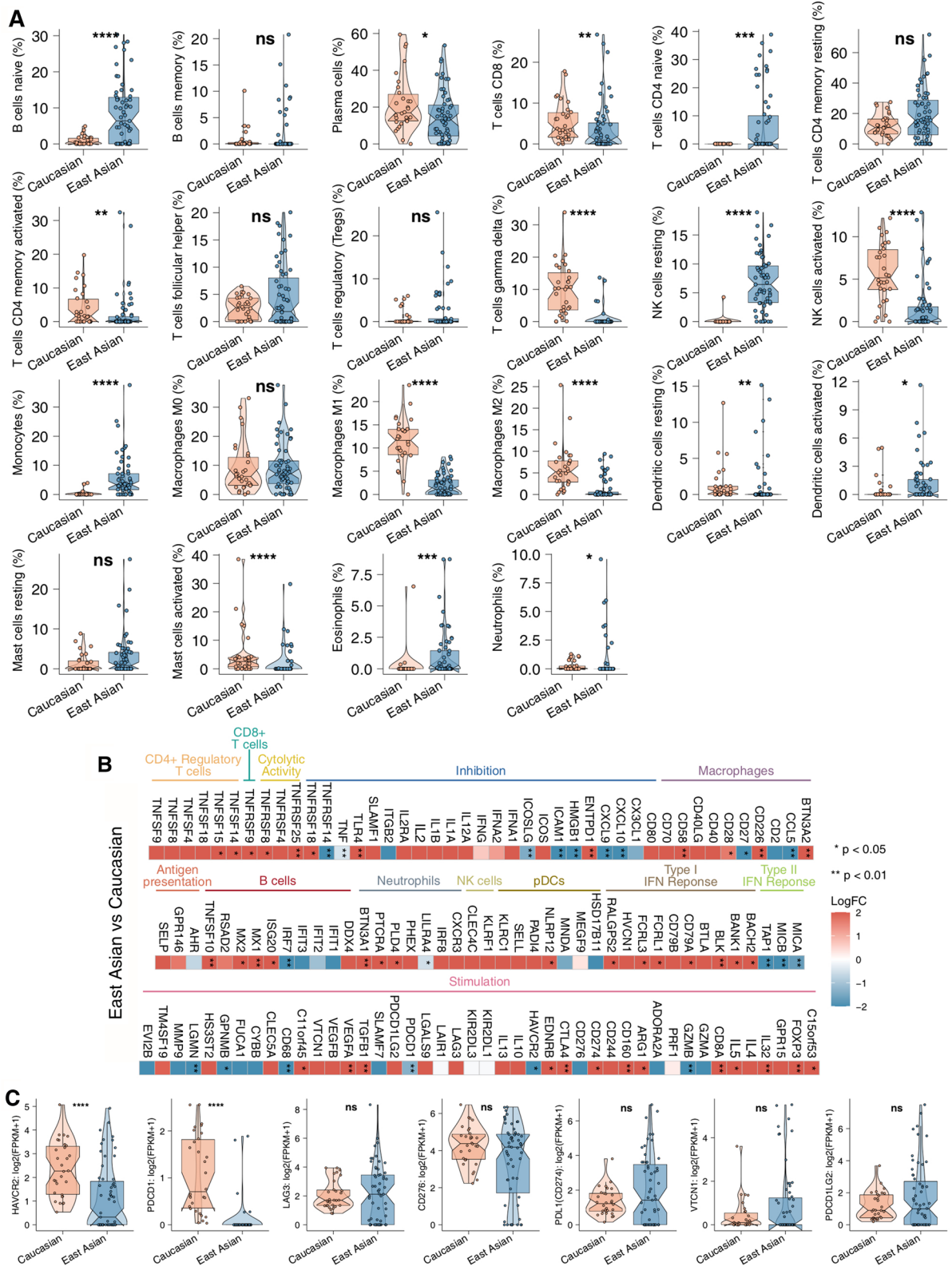


Fig. 6 (See legend on previous page.)

SCLC and were sensitive to standard therapies for SCLC [37–39].

This study is interesting given the critical role of *TP53/RB1* co-mutations in SCLC tumors. Compared to the *TP53/RB1* co-mutations in the Caucasian cohort, an 8% decrease in *TP53/RB1* co-mutations was identified in the EA cohort (67% vs 59%), which is consistent with results from other studies [1, 4, 40]. However, mutations, such as *TP53*, *RB1*, and *TP53/RB1* co-mutation, were not found to be significantly associated with clinical benefits in both the EA and Caucasian cohorts. A mutation in *OTOF*, a calcium-sensing protein triggering cell membrane fusion and regulating exocytosis, was significantly associated with poor OS in the Caucasian cohort [41, 42]. APC mutations were significantly correlated with shorter OS in the EA cohort, mediating faster tumorigenesis [43]. Mondaca et al. found that APC alterations were associated with the clinical outcomes of colorectal cancer patients [44]. Evidence has indicated that *NSD3* has crucial effects on cancer cell proliferation and invasion via multiple signaling pathways [45–47]. In the EA cohort, *NSD3* mutations were detected to be correlated with poor OS. Consistent with the previous study, *KDM5C* mutations had prognostic implications in EA SCLC patients [48]. A *GRM3* mutation was previously shown to upregulate MAPK pathway activity [49], and its presence was correlated with shorter survival. *CTNND1* was previously identified to bind and stabilize cadherins, further regulating Wnt/ β -catenin signaling pathway activity during tumor progression [50, 51], and the *CTNND1* mutation was associated with adverse OS in the EA cohort. *FANCG* was shown to play an important role in the activation of the Fanconi anemia (FA) pathway with the localization of the nuclear FA complex (including *FANCG*) [52], and it can also interact with *FANCD1* (*BRCA2*) [53, 54]. In our findings, we identified that a *FANCD1* mutation was associated with unfavorable OS in the EA SCLC cohort. In lung cancer, *MET* alterations have been suggested to be associated with a poor prognosis [55], and their presence was associated with shorter OS in the EA SCLC cohort. Long et al. reported that *COL6A6* interacted with *P4HA3* to suppress the growth and metastasis of pituitary adenoma via blocking the PI3K-Akt pathway [56]. Additionally, Qiao et al. indicated that *COL6A6* was a tumor suppressor gene in NSCLC and was involved in NSCLC tumorigenesis by regulating the JAK signalling pathway [57].

It is crucial to characterize the immunological profile of SCLC in the EA population, as this landscape might indicate the molecular mechanism of response, efficacy and resistance to specific immunotherapy and provide novel and potential implications of combination therapy. For example, high TMB and alterations in DDR were

previously identified to be strongly correlated with better survival in patients who underwent ICI treatments [11, 58, 59]. Through accumulating incorrect DNA damage, tumors harboring higher DDR mutations commonly had a higher TMB level [59]. Notably, significantly higher TMB levels were observed in the EA cohort (median 16.75 Mut/Mb; mean 30.95 Mut/Mb) than those in the Caucasian cohort (median 6.24 Mut/Mb; mean 7.03 Mut/Mb). Additionally, the number of DDR alterations was significantly higher in EA SCLC tumors than in Caucasian SCLC tumors. We found that high TMB was significantly positively correlated with high DDR alterations. Preclinical SCLC models were sensitive to PARP inhibition alone and the efficacy of chemotherapy was also enhanced by the addition of a PARP inhibitor [60]. Additionally, recent studies have shown that the efficacy of immunotherapy is related to a high TMB, high genomic instability, and high immunogenicity in tumor cells [61]. Moreover, a subset of patients responded to the anti-PD-1 agent nivolumab or pembrolizumab when administered as the third or later treatment line (response rates 12–20%) and experienced very prolonged responses, as median durations of response were 17.9 months and not-reached (after 7.7 months of follow-up), respectively [62, 63]. An important observation from this study is that East Asian SCLC patients have high mutation counts of DDR signaling pathways and TMB, which raises the question of combination approaches using PARPis and ICIs [64].

In addition to TMB and DDR alterations, the inflammatory gene expression profile (GEP), specific immune cells (e.g., CD4+ T cells, CD8+ T cells), and immune checkpoint expression levels played a critical role in SCLC treated with ICIs [11, 65]. Using the CIBERSORT algorithm, there were higher proportions of resting-type immune cells, such as naïve B cells, naïve CD4+ T cells, resting memory CD4+ T cells, resting NKs and resting DCs, in the EA SCLC cohort than in the Caucasian cohort. TGF- β signaling, containing *TGFBI*, has been reported to disrupt the recruitment and infiltration of CD8+ T cells into the center of tumors [66]. Treatment with PD-(L) 1 can facilitate T-cell infiltration, provoke antitumor immunity and attenuate tumor progression [66]. *FOXP3*, a conventional biomarker for regulatory T cells (Tregs), can attenuate effective T cell (Teff) activity and is associated with clinical benefits in several tumors [67–69]. Emerging studies have indicated that *VEGFA* overexpression tends to involve a suppressive tumor microenvironment (TME) and decreased antitumor immunity [70, 71], further mediating primary resistance to the anti-PD-(L) 1 regimen. Here, we discovered that there was a high expression level of several suppressive mediators, such as *VEGFA*, *TGFBI* and *FOXP3*, in the EA cohort.

In contrast, chemokines (*CXCL9* and *CXCL10*) and a cytolytic activity-related gene (*GZMB*) were commonly downregulated in the EA cohort. Chemokines, such as *CXCL9* and *CXCL10*, serve as key factors that recruit T cells into the center of the tumor, further promoting antitumor immunity and disrupting tumor cell proliferation and invasion [11, 72–74].

Using the CMap algorithm, we identified potential inhibitors/compounds that may be capable of targeting *TP53/RB1* co-mutations, such as the topoisomerase inhibitors mitoxantrone and irinotecan, the HSP inhibitor alvespimycin, and the PARPi NU-1025. Alterations in DDR signaling pathways have significance in the usage of genotoxic agents, such as platinum-based chemotherapy and PARPi [75–78]. Additionally, unrepaired DNA mediates immune priming by multiple molecular mechanisms and upregulates PD-(L) 1 expression [79]. Furthermore, PARPi was involved in the development of the inflammatory TME and further promoted a productive immune response [79–81].

However, this study had certain limitations. First, due to the limited number of Caucasian SCLC patients, this finding might need a large population for validation. Second, intratumor heterogeneity was a crucial metric for tumor evolution, but our analyses were based only on single biopsies/samples; therefore, our findings cannot portray the whole evolution of SCLC. Third, this study lacks copy number variation and proteomics analyses to validate our findings. Finally, animal and laboratory experiments are necessary to further illustrate and validate our findings.

Conclusions

In summary, the present findings portray the clinical, immunological, and genomic profile differences among EA and Caucasian SCLC patients and might provide clinical implications for EA SCLC patients with novel alterations, potential biological signaling pathways and new immunological factors to target.

Abbreviations

SCLC: Small-cell lung cancer; EA: East Asian TMB: tumor mutation burden; EMT: Epithelial-mesenchymal transition; OS: Overall survival ICI: immune checkpoint inhibitors; TME: Tumor microenvironment; WES: Whole-exome sequencing; IRBs: Institutional Review Boards; RNA-seq: RNA sequencing; GDSC: Genomics of Drug Sensitivity in Cancer; DDR: DNA damage response; ssGSEA: Single-sample gene set enrichment analysis; NCG: Network of Cancer Genes; CMap: Connectivity Map; MoA: Mechanism of action; GSEA: Gene set enrichment analysis; FDR: False discovery rate; SNPs: Single-nucleotide polymorphisms; SNV: Single-nucleotide variant; TSGs: Tumor suppressor genes; HR: Homologous recombination; SSB: Single-strand breaks; NHEJ: Non-homologous end joining; NER: Nucleotide excision repair; BER: Base excision repair; HSP: Heat shock protein; PARPi: PARP inhibitor; DCs: Dendritic cells; NKs: Natural killer cells.

Supplementary Information

The online version contains supplementary material available at <https://doi.org/10.1186/s12935-022-02588-w>.

Additional file 1: Figure S1. Related to Fig. 1c–d; heatmap showing mutually exclusive and co-occurring mutations in the East Asian (a) and Caucasian (b) cohorts.

Additional file 2: Figure S2. Related to Fig. 3c; heatmap showing mutually exclusive and co-occurring mutations in the East Asian (a) and Caucasian (b) cohorts.

Additional file 3: Figure S3. Related to Fig. 4; the correlation between the ssGSEA scores of each DDR signaling pathway and TMB in the East Asian (a) and Caucasian (b) cohorts.

Additional file 4: Figure S4. Top 20 mutated drivers and alterations in several key biological pathways in SCLC. An overview of the top 20 mutated driver genes in the East Asian (a) and Caucasian (b) cohorts. c Significantly mutated genes in the key biological signaling pathways between the East Asian and Caucasian cohorts.

Additional file 5: Figure S5. The distinct prognosis of significant driver gene mutations in SCLC. The univariable Cox regression model includes clinical characteristics and driver gene mutations (mutation rate $\geq 10\%$) in the East Asian (a) and Caucasian (b) cohorts. Several driver gene mutations (mutation rate $\geq 10\%$) were associated with a distinct prognosis between the East Asian (c) and Caucasian (d) cohorts.

Additional file 6: Figure S6. Related to Additional file 5: Fig. S5; heatmap depicting the mean differences in drug sensitivity (GDSC database) between the top 20 mutated genes and the corresponding wild-type gene in the East Asian (a) and Caucasian (b) cohorts. The y-axis indicates different drugs in the GDSC database, and the x-axis of the heatmap indicates different mutation statuses of the top 20 mutated genes. Red indicates upregulation, while blue indicates downregulation.

Additional file 7: Figure S7. Related to Fig. 6a; heatmap depicting the mean differences in the contents of 22 immune cells between different clinical characteristics and mutation status in the East Asian (a) and Caucasian (b) cohorts. The y-axis indicates different immune cells calculated by the CIBERSORT algorithm, and the x-axis of the heatmap indicates clinical characteristics and mutation status. Red indicates upregulation, while blue indicates downregulation.

Additional file 8: Figure S8. Related to Fig. 6b; heatmap depicting the mean differences in the contents of immune-related gene mRNA expression between different clinical characteristics and mutation statuses in the East Asian (a) and Caucasian (b) cohorts. The y-axis indicates immune-related gene mRNA expression, and the x-axis of the heatmap indicates clinical characteristics and mutation status. Red indicates upregulation, while blue indicates downregulation.

Additional file 9: Figure S9. Heatmap depicting the correlation ρ between the proportion of immune cells and mutations in each DDR pathway and TMB in the East Asian (a) and Caucasian (b) cohorts.

Additional file 10: Table S1. Related to Additional file 1: Fig. S1a. The results of co-occurrence/mutual exclusivity of oncogenes/TSGs in the East Asian cohort (Top20 mutated genes).

Additional file 11: Table S2. Related to Additional file 1: Fig. S1b. The results of the co-occurrence/mutual exclusivity of oncogenes/TSGs in the Caucasian cohort (Top20 mutated genes).

Additional file 12: Table S3. Related to Additional file 2: Fig. S2a. The results of the co-occurrence/mutual exclusivity of oncogenes/TSGs in the East Asian cohort (significantly mutated driver genes).

Additional file 13: Table S4. Related to Additional file 2: Fig. S2b. The results of the co-occurrence/mutual exclusivity of oncogenes/TSGs in the Caucasian cohort (significantly mutated driver genes).

Additional file 14: Table S5. Related to Additional file 5: Fig. S5a. The results of the CMap analysis of the East Asian cohort (*TP53/RB1* co-mutations vs No alterations in *TP53/RB1*).

Additional file 15: Table S6. Related to Additional file 5: Fig. S5a The results of the CMap analysis of the Caucasian cohort (TP53/RB1 co-mutations vs No alterations in TP53/RB1).

Additional file 16: Supplemental methods.

Acknowledgements

Not applicable.

Author contributions

Conceptualization, PL, JZ; Formal analysis, AQL; Software, AQL, NNZ, WLZ and JXZ; Supervision, PL, JZ; Resources, PL, JZ and AQL; Visualization, AQL, TW; Writing—original draft, AQL, NNZ, WLZ, JXZ, TW and LLG; Writing—review & editing, AQL, NNZ, WLZ, JXZ, TW and LLG. All authors read and approved the final manuscript.

Funding

This work was supported by the Natural Science Foundation of Guangdong Province (Grant No. 2018A030313846 and 2021A1515012593), the Science and Technology Planning Project of Guangdong Province (Grant No. 2019A030317020), the Science and Technology Program of Guangzhou (201803010024), and the National Natural Science Foundation of China (Grant No. 81802257, 81871859, 81772457, 82172750 and 82172811).

Availability of data and materials

All the data generated or analyzed during this study are included in this published article (https://www.cbiportal.org/study/summary?id=scl_c_ucolo_gne_2015) and our supplementary files. All other relevant data are available from the authors of this study upon request.

Declarations

Ethics approval and consent to participate

The patients/participants provided their written informed consent to participate in this study and the research presented here has been performed in accordance with the Declaration of Helsinki and has been approved by the ethics committee of the First Affiliated Hospital of Guangzhou Medical University, the Sun Yat-sen University Cancer Center, and the Zhujiang Hospital of Southern Medical University.

Consent for publication

Not applicable.

Competing interests

The authors declared no competing interests for this work.

Author details

¹Department of Oncology, Zhujiang Hospital, Southern Medical University, 253 Industrial Avenue, Guangzhou 510282, Guangdong, China. ²Department of Medical Oncology, State Key Laboratory of Oncology in South China, Collaborative Innovation Center for Cancer Medicine, Sun Yat-Sen University Cancer Center, Guangzhou, China. ³Department of Medicine, National Clinical Research Center for Respiratory Disease, State Key Laboratory of Respiratory Disease, Guangzhou Institute of Respiratory Disease, Guangzhou, China. ⁴Department of Pathology, Zhujiang Hospital, Southern Medical University, Guangzhou, Guangdong, China.

Received: 26 February 2022 Accepted: 12 April 2022

Published online: 29 April 2022

References

- George J, Lim JS, Jang SJ, Cun Y, Ozretić L, Kong G, Leenders F, Lu X, Fernández-Cuesta L, Bosco G, et al. Comprehensive genomic profiles of small cell lung cancer. *Nature*. 2015;524:47–53. <https://doi.org/10.1038/nature14664>.
- Li M, Lin A, Luo P, Shen W, Xiao D, Gou L, Zhang J, Guo L. DNAH10 mutation correlates with cisplatin sensitivity and tumor mutation burden in small-cell lung cancer. *Aging (Albany NY)*. 2020;12:1285–303. <https://doi.org/10.18632/aging.102683>.
- Rudin CM, Poirier JT, Byers LA, Dive C, Dowlati A, George J, Heymach JV, Johnson JE, Lehman JM, MacPherson D, et al. Molecular subtypes of small cell lung cancer: a synthesis of human and mouse model data. *Nat Rev Cancer*. 2019;19:289–97. <https://doi.org/10.1038/s41568-019-0133-9>.
- Hu J, Wang Y, Zhang Y, Yu Y, Chen H, Liu K, Yao M, Wang K, Gu W, Shou T. Comprehensive genomic profiling of small cell lung cancer in Chinese patients and the implications for therapeutic potential. *Cancer Med*. 2019;8:4338–47. <https://doi.org/10.1002/cam4.2199>.
- Nong J, Gong Y, Guan Y, Yi X, Yi Y, Chang L, Yang L, Lv J, Guo Z, Jia H, et al. Circulating tumor DNA analysis depicts subclonal architecture and genomic evolution of small cell lung cancer. *Nat Commun*. 2018;9:3114. <https://doi.org/10.1038/s41467-018-05327-w>.
- Jiang L, Huang J, Higgs BW, Hu Z, Xiao Z, Yao X, Conley S, Zhong H, Liu Z, Brohawn P, et al. Genomic landscape survey identifies SRSF1 as a key oncogene in small cell lung cancer. *PLoS Genet*. 2016;12:e1005895. <https://doi.org/10.1371/journal.pgen.1005895>.
- Umemura S, Mimaki S, Makinoshima H, Tada S, Ishii G, Ohmatsu H, Niho S, Yoh K, Matsumoto S, Takahashi A, et al. Therapeutic priority of the PI3K/AKT/mTOR pathway in small cell lung cancers as revealed by a comprehensive genomic analysis. *J Thorac Oncol Off Publ Int Assoc Study Lung Cancer*. 2014;9:1324–31. <https://doi.org/10.1097/JTO.0000000000000250>.
- Wang Z, Jiang Z, Lu H. Molecular genetic profiling of small cell lung carcinoma in a Chinese cohort. *Transl Cancer Res*. 2019;8:255–61. <https://doi.org/10.21037/tcr.2019.01.26>.
- Karachaliou N, Sosa AE, Rosell R. Unraveling the genomic complexity of small cell lung cancer. *Transl lung cancer Res*. 2016;5:363–6. <https://doi.org/10.21037/tlcr.2016.07.02>.
- Horn L, Mansfield AS, Szczesna A, Havel L, Krzakowski M, Hochmair MJ, Huemer F, Losonczy G, Johnson ML, Nishio M, et al. First-line Atezolizumab plus chemotherapy in extensive-stage small-cell lung cancer. *N Engl J Med*. 2018;379:2220–9. <https://doi.org/10.1056/NEJMoa1809064>.
- Hellmann MD, Nathanson T, Rizvi H, Creelan BC, Sanchez-Vega F, Ahuja A, Ni A, Novik JB, Mangarin LMB, Abu-Akeel M, et al. Genomic features of response to combination immunotherapy in patients with advanced non-small-cell lung cancer. *Cancer Cell*. 2018;33:843–852.e4. <https://doi.org/10.1016/j.ccell.2018.03.018>.
- Yang W, Soares J, Greninger P, Edelman EJ, Lightfoot H, Forbes S, Bindal N, Beare D, Smith JA, Thompson IR, et al. Genomics of Drug Sensitivity in Cancer (GDSC): a resource for therapeutic biomarker discovery in cancer cells. *Nucleic Acids Res*. 2013;41:D955–61. <https://doi.org/10.1093/nar/gks1111>.
- Newman AM, Liu CL, Green MR, Gentles AJ, Feng W, Xu Y, Hoang CD, Diehn M, Alizadeh AA. Robust enumeration of cell subsets from tissue expression profiles. *Nat Methods*. 2015;12:453–7. <https://doi.org/10.1038/nmeth.3337>.
- Rooney MS, Shukla SA, Wu CJ, Getz G, Hacohen N. Molecular and genetic properties of tumors associated with local immune cytolytic activity. *Cell*. 2015;160:48–61. <https://doi.org/10.1016/j.cell.2014.12.033>.
- Thorsson V, Gibbs DL, Brown SD, Wolf D, Bortone DS, Ou Yang T-H, Porta-Pardo E, Gao GF, Plaisier CL, Eddy JA, et al. The immune landscape of cancer. *Immunity*. 2018;48:812–830.e14. <https://doi.org/10.1016/j.immuni.2018.03.023>.
- Gu Z, Eils R, Schlesner M. Complex heatmaps reveal patterns and correlations in multidimensional genomic data. *Bioinformatics*. 2016;32:2847–9. <https://doi.org/10.1093/bioinformatics/btw313>.
- Mayakonda A, Lin D-C, Assenov Y, Plass C, Koeffler HP. Maftools: efficient and comprehensive analysis of somatic variants in cancer. *Genome Res*. 2018;28:1747–56. <https://doi.org/10.1101/gr.239244.118>.
- Chalmers ZR, Connelly CF, Fabrizio D, Gay L, Ali SM, Ennis R, Schrock A, Campbell B, Shlien A, Chmielecki J, et al. Analysis of 100,000 human cancer genomes reveals the landscape of tumor mutational burden. *Genome Med*. 2017;9:34. <https://doi.org/10.1186/s13073-017-0424-2>.
- Liberzon A, Subramanian A, Pinchback R, Thorvaldsdottir H, Tamayo P, Mesirov JP. Molecular signatures database (MSigDB) 3.0. *Bioinformatics*. 2011;27:1739–40. <https://doi.org/10.1093/bioinformatics/btr260>.
- Hänzelmann S, Castelo R, Guinney J. GSEA: gene set variation analysis for microarray and RNA-seq data. *BMC Bioinformatics*. 2013;14:7. <https://doi.org/10.1186/1471-2105-14-7>.

21. Repana D, Nulsen J, Dressler L, Bortolomeazzi M, Venkata SK, Tourna A, Yakovleva A, Palmieri T, Ciccarelli FD. The Network of Cancer Genes (NCG): a comprehensive catalogue of known and candidate cancer genes from cancer sequencing screens. *Genome Biol.* 2019;20:1. <https://doi.org/10.1186/s13059-018-1612-0>.
22. Lamb J, Crawford ED, Peck D, Modell JW, Blat IC, Wrobel MJ, Lerner J, Brunet J-P, Subramanian A, Ross KN, et al. The Connectivity Map: using gene-expression signatures to connect small molecules, genes, and disease. *Science.* 2006;313:1929–35. <https://doi.org/10.1126/science.1132939>.
23. Subramanian A, Narayan R, Corsello SM, Peck DD, Natoli TE, Lu X, Gould J, Davis JF, Tubelli AA, Asiedu JK, et al. A Next Generation Connectivity Map: L1000 Platform and the First 1,000,000 Profiles. *Cell.* 2017;171:1437–1452. e17. <https://doi.org/10.1016/j.cell.2017.10.049>.
24. Benjamin D, Sato T, Cibulskis K, Getz G, Stewart C, Lichtenstein L. Calling somatic SNVs and indels with mutect2. *bioRxiv.* 2019. <https://doi.org/10.1101/861054>.
25. Salerno EP, Bedognetti D, Mauldin IS, Deacon DH, Shea SM, Pinczewski J, Obeid JM, Coukos G, Wang E, Gajewski TF, et al. Human melanomas and ovarian cancers overexpressing mechanical barrier molecule genes lack immune signatures and have increased patient mortality risk. *Oncoimmunology.* 2016;5:e1240857. <https://doi.org/10.1080/2162402X.2016.1240857>.
26. Zhao Y, Li D, Zhao J, Song J, Zhao Y. The role of the low-density lipoprotein receptor-related protein 1 (LRP-1) in regulating blood-brain barrier integrity. *Rev Neurosci.* 2016;27:623–34. <https://doi.org/10.1515/revneuro-2015-0069>.
27. Tabouret E, Labussière M, Alentorn A, Schmitt Y, Marie Y, Sanson M. LRP1B deletion is associated with poor outcome for glioblastoma patients. *J Neurol Sci.* 2015;358:440–3. <https://doi.org/10.1016/j.jns.2015.09.345>.
28. Streppel MM, Vincent A, Mukherjee R, Campbell NR, Chen S-H, Konstantopoulos K, Goggins MG, Van Seuning I, Maitra A, Montgomery EA. Mucin 16 (cancer antigen 125) expression in human tissues and cell lines and correlation with clinical outcome in adenocarcinomas of the pancreas, esophagus, stomach, and colon. *Hum Pathol.* 2012;43:1755–63. <https://doi.org/10.1016/j.humpath.2012.01.005>.
29. Ge W, Hu H, Cai W, Xu J, Hu W, Weng X, Qin X, Huang Y, Han W, Hu Y, et al. High-risk Stage III colon cancer patients identified by a novel five-gene mutational signature are characterized by upregulation of IL-23A and gut bacterial translocation of the tumor microenvironment. *Int J cancer.* 2020;146:2027–35. <https://doi.org/10.1002/ijc.32775>.
30. Aboubakar Nana F, Vanderputten M, Ocak S. Role of focal adhesion kinase in small-cell lung cancer and its potential as a therapeutic target. *Cancers (Basel).* 2019;11:1683. <https://doi.org/10.3390/cancers11111683>.
31. Avizienyte E, Frame MC. Src and FAK signalling controls adhesion fate and the epithelial-to-mesenchymal transition. *Curr Opin Cell Biol.* 2005;17:542–7. <https://doi.org/10.1016/j.ceb.2005.08.007>.
32. Lu W, Kang Y. Epithelial-mesenchymal plasticity in cancer progression and metastasis. *Dev Cell.* 2019;49:361–74. <https://doi.org/10.1016/j.devcel.2019.04.010>.
33. Schulze AB, Evers G, Kerkhoff A, Mohr M, Schliemann C, Berdel WE, Schmidt LH. Future options of molecular-targeted therapy in small cell lung cancer. *Cancers (Basel).* 2019. <https://doi.org/10.3390/cancers11050690>.
34. Augert A, Zhang Q, Bates B, Cui M, Wang X, Wildey G, Dowlati A, MacPherson D. Small cell lung cancer exhibits frequent inactivating mutations in the histone methyltransferase KMT2D/MLL2: CALGB 151111 (Alliance). *J Thorac Oncol Off Publ Int Assoc Study Lung Cancer.* 2017;12:704–13. <https://doi.org/10.1016/j.jtho.2016.12.011>.
35. Jia D, Augert A, Kim D-W, Eastwood E, Wu N, Ibrahim AH, Kim K-B, Dunn CT, Pillai SPS, Gazdar AF, et al. Crebbp loss drives small cell lung cancer and increases sensitivity to hdac inhibition. *Cancer Discov.* 2018;8:1422–37. <https://doi.org/10.1158/2159-8290.CD-18-0385>.
36. Hellwig M, Merk DJ, Lutz B, Schüller U. Preferential sensitivity to HDAC inhibitors in tumors with CREBBP mutation. *Cancer Gene Ther.* 2020;27:294–300. <https://doi.org/10.1038/s41417-019-0099-5>.
37. Sequist LV, Waltman BA, Dias-Santagata D, Digumarthy S, Turke AB, Fidias P, Bergtson K, Shaw AT, Gettinger S, Cosper AK, et al. Genotypic and histological evolution of lung cancers acquiring resistance to EGFR inhibitors. *Sci Transl Med.* 2011;3:7526. <https://doi.org/10.1126/scitranslmed.3002003>.
38. Ma S, He Z, Fu H, Wang L, Wu X, Zhang Z, Wang Q. Dynamic changes of acquired T790M mutation and small cell lung cancer transformation in a patient with EGFR-mutant adenocarcinoma after first- and third-generation EGFR-TKIs: a case report. *Transl Lung Cancer Res.* 2020;9:139–43. <https://doi.org/10.21037/tlcr.2020.01.07>.
39. Wei T, Zhu W, Fang S, Zeng X, Huang J, Yang J, Zhang J, Guo L. miR-495 promotes the chemoresistance of SCLC through the epithelial-mesenchymal transition via Etk/BMX. *Am J Cancer Res.* 2017;7:628–46.
40. Qiu Z, Zhu W, Meng H, Tong L, Li X, Luo P, Yi L, Zhang X, Guo L, Wei T, et al. CDYL promotes the chemoresistance of small cell lung cancer by regulating H3K27 trimethylation at the CDKN1C promoter. *Theranostics.* 2019;9:4717–29. <https://doi.org/10.7150/thno.33680>.
41. Jiao X, Wood LD, Lindman M, Jones S, Buckhaults P, Polyak K, Sukumar S, Carter H, Kim D, Karchin R, et al. Somatic mutations in the Notch, NF- κ B, PIK3CA, and Hedgehog pathways in human breast cancers. *Genes Chromosom Cancer.* 2012;51:480–9. <https://doi.org/10.1002/gcc.21935>.
42. Zhuo E, He J, Wei T, Zhu W, Meng H, Li Y, Guo L, Zhang J. Down-regulation of GnT-V enhances nasopharyngeal carcinoma cell CNE-2 radiosensitivity in vitro and in vivo. *Biochem Biophys Res Commun.* 2012;424:554–62. <https://doi.org/10.1016/j.bbrc.2012.07.001>.
43. Huels DJ, Bruens L, Hodder MC, Cammareri P, Campbell AD, Ridgway RA, Gay DM, Solar-Aboud M, Faller WJ, Nixon C, et al. Wnt ligands influence tumour initiation by controlling the number of intestinal stem cells. *Nat Commun.* 2018;9:1132. <https://doi.org/10.1038/s41467-018-03426-2>.
44. Mondaca S, Walch H, Nandakumar S, Chatila WK, Schultz N, Yaeger R. Specific mutations in APC, but not alterations in DNA damage response, associate with outcomes of patients with metastatic colorectal cancer. *Gastroenterology.* 2020. <https://doi.org/10.1053/j.gastro.2020.07.041>.
45. Vougiouklakis T, Hamamoto R, Nakamura Y, Saloura V. The NSD family of protein methyltransferases in human cancer. *Epigenomics.* 2015;7:863–74. <https://doi.org/10.2217/epi.15.32>.
46. Bennett RL, Swaroop A, Troche C, Licht JD. The role of nuclear receptor-binding set domain family histone lysine methyltransferases in cancer. *Cold Spring Harb Perspect Med.* 2017. <https://doi.org/10.1101/cshperspect.a026708>.
47. Tong L, Luo Y, Wei T, Guo L, Wang H, Zhu W, Zhang J. KH-type splicing regulatory protein (KHSRP) contributes to tumorigenesis by promoting miR-26a maturation in small cell lung cancer. *Mol Cell Biochem.* 2016;422:61–74. <https://doi.org/10.1007/s11010-016-2806-y>.
48. Voss MH, Reising A, Cheng Y, Patel P, Marker M, Kuo F, Chan TA, Choueiri TK, Hsieh JJ, Hakimi AA, et al. Genomically annotated risk model for advanced renal-cell carcinoma: a retrospective cohort study. *Lancet Oncol.* 2018;19:1688–98. [https://doi.org/10.1016/S1470-2045\(18\)30648-X](https://doi.org/10.1016/S1470-2045(18)30648-X).
49. Neto A, Ceol CJ. Melanoma-associated GRM3 variants dysregulate melanosome trafficking and cAMP signaling. *Pigment Cell Melanoma Res.* 2018;31:115–9. <https://doi.org/10.1111/pcmr.12610>.
50. Tang B, Tang F, Wang Z, Qi G, Liang X, Li B, Yuan S, Liu J, Yu S, He S. Over-expression of CTNND1 in hepatocellular carcinoma promotes carcinous characters through activation of Wnt/ β -catenin signaling. *J Exp Clin Cancer Res.* 2016;35:82. <https://doi.org/10.1186/s13046-016-0344-9>.
51. Zhang Z, Zhu W, Zhang J, Guo L. Tyrosine kinase Etk/BMX protects nasopharyngeal carcinoma cells from apoptosis induced by radiation. *Cancer Biol Ther.* 2011;11:690–8. <https://doi.org/10.4161/cbt.11.7.15060>.
52. Jeong E, Lee S-G, Kim H-S, Yang J, Shin J, Kim Y, Kim J, Schärer OD, Kim Y, Yeo J-E, et al. Structural basis of the fanconi anemia-associated mutations within the FANCA and FANCG complex. *Nucleic Acids Res.* 2020;48:3328–42. <https://doi.org/10.1093/nar/gkaa062>.
53. Schubert S, van Luttikhuisen JL, Auber B, Schmidt G, Hofmann W, Penkert J, Davenport CF, Hille-Betz U, Wendeburg L, Bublitz J, et al. The identification of pathogenic variants in BRCA1/2 negative, high risk, hereditary breast and/or ovarian cancer patients: high frequency of FANCM pathogenic variants. *Int J cancer.* 2019;144:2683–94. <https://doi.org/10.1002/ijc.31992>.
54. He Y, Zhang J, Zhang J, Yuan Y. The role of c-myc in regulating mdr1 gene expression in tumor cell line KB. *Chin Med J (Engl).* 2000;113:848–51.
55. Reis H, Metznermacher M, Goetz M, Savvidou N, Darwiche K, Aigner C, Herold T, Eberhardt WE, Skiba C, Hense J, et al. MET expression in advanced non-small-cell lung cancer: effect on clinical outcomes of

- chemotherapy, targeted therapy, and immunotherapy. *Clin Lung Cancer*. 2018;19:e441–63. <https://doi.org/10.1016/j.clcc.2018.03.010>.
56. Long R, Liu Z, Li J, Yu H. COL6A6 interacted with P4HA3 to suppress the growth and metastasis of pituitary adenoma via blocking PI3K-Akt pathway. *Aging (Albany NY)*. 2019;11:8845–59. <https://doi.org/10.18632/aging.102300>.
 57. Qiao H, Feng Y, Tang H. COL6A6 inhibits the proliferation and metastasis of non-small cell lung cancer through the JAK signalling pathway. *Transl Cancer Res*. 2021;10:4514–22. <https://doi.org/10.21037/tcr-21-2002>.
 58. Zhang J, Zhou N, Lin A, Luo P, Chen X, Deng H, Kang S, Guo L, Zhu W, Zhang J. ZFH3 mutation as a protective biomarker for immune checkpoint blockade in non-small cell lung cancer. *Cancer Immunol Immunother*. 2021;70:137–51. <https://doi.org/10.1007/s00262-020-02668-8>.
 59. Luo P, Lin A, Li K, Wei T, Zhang J. DDR pathway alteration, tumor mutation burden, and cisplatin sensitivity in small cell lung cancer: difference detected by whole exome and targeted gene sequencing. *J Thorac Oncol Off Publ Int Assoc Study Lung Cancer*. 2019;14:e276–9. <https://doi.org/10.1016/j.jtho.2019.08.2509>.
 60. Byers LA, Wang J, Nilsson MB, Fujimoto J, Saintigny P, Yordy J, Giri U, Peyton M, Fan YH, Diao L, et al. Proteomic profiling identifies dysregulated pathways in small cell lung cancer and novel therapeutic targets including PARP1. *Cancer Discov*. 2012;2:798–811. <https://doi.org/10.1158/2159-8290.CD-12-0112>.
 61. Ma X, Wang S, Zhang Y, Wei H, Yu J. Efficacy and safety of immune checkpoint inhibitors (ICIs) in extensive-stage small cell lung cancer (SCLC). *J Cancer Res Clin Oncol*. 2021;147:593–606. <https://doi.org/10.1007/s00432-020-03362-z>.
 62. Ready N, Farago AF, de Braud F, Atmaca A, Hellmann MD, Schneider JG, Spigel DR, Moreno V, Chau I, Hann CL, et al. Third-Line nivolumab monotherapy in recurrent SCLC: CheckMate 032. *J Thorac Oncol Off Publ Int Assoc Study Lung Cancer*. 2019;14:237–44. <https://doi.org/10.1016/j.jtho.2018.10.003>.
 63. Chung HC, Piha-Paul SA, Lopez-Martin J, Schellens JHM, Kao S, Miller WHJ, Delord J-P, Gao B, Planchard D, Gottfried M, et al. Pembrolizumab after two or more lines of previous therapy in patients with recurrent or metastatic SCLC: results from the KEYNOTE-028 and KEYNOTE-158 studies. *J Thorac Oncol Off Publ Int Assoc Study Lung Cancer*. 2020;15:618–27. <https://doi.org/10.1016/j.jtho.2019.12.109>.
 64. Arulananda S, Mitchell P, John T. DDR alterations as a surrogate marker for TMB in SCLC—Use it or Lose it? *J Thorac Oncol Off Publ Int Assoc Study Lung Cancer*. 2019;14:1498–500. <https://doi.org/10.1016/j.jtho.2019.06.025>.
 65. Lin A, Wei T, Meng H, Luo P, Zhang J. Role of the dynamic tumor microenvironment in controversies regarding immune checkpoint inhibitors for the treatment of non-small cell lung cancer (NSCLC) with EGFR mutations. *Mol Cancer*. 2019;18:139. <https://doi.org/10.1186/s12943-019-1062-7>.
 66. Mariathasan S, Turley SJ, Nickles D, Castiglioni A, Yuen K, Wang Y, Kadel EEIII, Koepfen H, Astarita JL, Cubas R, et al. TGFβ attenuates tumour response to PD-L1 blockade by contributing to exclusion of T cells. *Nature*. 2018;554:544–8. <https://doi.org/10.1038/nature25501>.
 67. Kurose K, Ohue Y, Wada H, Iida S, Ishida T, Kojima T, Doi T, Suzuki S, Isobe M, Funakoshi T, et al. Phase Ia study of FoxP3+ CD4 Treg depletion by infusion of a humanized Anti-CCR4 antibody, KW-0761, in cancer patients. *Clin cancer Res an Off J Am Assoc Cancer Res*. 2015;21:4327–36. <https://doi.org/10.1158/1078-0432.CCR-15-0357>.
 68. Whiteside TL. FOXP3+ Treg as a therapeutic target for promoting anti-tumor immunity. *Expert Opin Ther Targets*. 2018;22:353–63. <https://doi.org/10.1080/14728222.2018.1451514>.
 69. Yi L, Fan J, Qian R, Luo P, Zhang J. Efficacy and safety of osimertinib in treating EGFR-mutated advanced NSCLC: a meta-analysis. *Int J cancer*. 2019;145:284–94. <https://doi.org/10.1002/ijc.32097>.
 70. Haratani K, Hayashi H, Takahama T, Nakamura Y, Tomida S, Yoshida T, Chiba Y, Sawada T, Sakai K, Fujita Y, et al. Clinical and immune profiling for cancer of unknown primary site. *J Immunother cancer*. 2019;7:251. <https://doi.org/10.1186/s40425-019-0720-z>.
 71. Wang Q, Gao J, Di W, Wu X. Anti-angiogenesis therapy overcomes the innate resistance to PD-1/PD-L1 blockade in VEGFA-overexpressed mouse tumor models. *Cancer Immunol Immunother*. 2020;69:1781–99. <https://doi.org/10.1007/s00262-020-02576-x>.
 72. Zhang X-C, Wang J, Shao G-G, Wang Q, Qu X, Wang B, Moy C, Fan Y, Albertyn Z, Huang X, et al. Comprehensive genomic and immunological characterization of Chinese non-small cell lung cancer patients. *Nat Commun*. 2019;10:1772. <https://doi.org/10.1038/s41467-019-09762-1>.
 73. Luo P, Lin A, Zhang J. Crosstalk between the MSI status and tumor micro-environment in colorectal cancer. *J Clin Oncol*. 2020;38:e15236–e15236. https://doi.org/10.1200/JCO.2020.38.15_suppl.e15236.
 74. Qiu Z, Lin A, Li K, Lin W, Wang Q, Wei T, Zhu W, Luo P, Zhang J. A novel mutation panel for predicting etoposide resistance in small-cell lung cancer. *Drug Des Devel Ther*. 2019;13:2021–41. <https://doi.org/10.2147/DDDT.S205633>.
 75. Kubelac P, Genestie C, Auguste A, Mesnage S, Le Formal A, Pautier P, Gouy S, Morice P, Bentivegna E, Maulard A, et al. Changes in dna damage response markers with treatment in advanced ovarian cancer. *Cancers (Basel)*. 2020;12:707. <https://doi.org/10.3390/cancers12030707>.
 76. Gee ME, Faraahi Z, McCormick A, Edmondson RJ. DNA damage repair in ovarian cancer: unlocking the heterogeneity. *J Ovarian Res*. 2018;11:50. <https://doi.org/10.1186/s13048-018-0424-x>.
 77. McMullen M, Karakasis K, Madariaga A, Oza AM. Overcoming platinum and PARP-inhibitor resistance in ovarian cancer. *Cancers (Basel)*. 2020;12:1607. <https://doi.org/10.3390/cancers12061607>.
 78. Zhao Y, Chen W, Zhu W, Meng H, Chen J, Zhang J. Overexpression of Interferon Regulatory Factor 7 (IRF7) reduces bone metastasis of prostate cancer cells in mice. *Oncol Res*. 2017;25:511–22. <https://doi.org/10.37277/096504016X14756226781802>.
 79. Stewart RA, Pilié PG, Yap TA. Development of PARP and immune-checkpoint inhibitor combinations. *Cancer Res*. 2018;78:6717–25. <https://doi.org/10.1158/0008-5472.CAN-18-2652>.
 80. Peyraud F, Italiano A. Combined PARP inhibition and immune checkpoint therapy in solid tumors. *Cancers (Basel)*. 2020;12:1502. <https://doi.org/10.3390/cancers12061502>.
 81. Fan J, Fong T, Xia Z, Zhang J, Luo P. The efficacy and safety of ALK inhibitors in the treatment of ALK-positive non-small cell lung cancer: a network meta-analysis. *Cancer Med*. 2018;7:4993–5005. <https://doi.org/10.1002/cam4.1768>.

Publisher's Note

Springer Nature remains neutral with regard to jurisdictional claims in published maps and institutional affiliations.

Ready to submit your research? Choose BMC and benefit from:

- fast, convenient online submission
- thorough peer review by experienced researchers in your field
- rapid publication on acceptance
- support for research data, including large and complex data types
- gold Open Access which fosters wider collaboration and increased citations
- maximum visibility for your research: over 100M website views per year

At BMC, research is always in progress.

Learn more biomedcentral.com/submissions

